Equation of state of supernova matter

C. Das and R. Sahu[*]
Department of Physics, Berhampur University, Berhampur-760007, Orissa, India

A. Mishra
Prananath Autonomous College, Khurda, India
(Received 2 May 2006; published 25 January 2007)

The equation of state (EOS) of dense supernova matter composed of protons, neutrons, and relativistic electrons is calculated within finite temperature Brueckner Goldstone approach with effective two-body Sussex interaction and compared with asymmetric nuclear matter. Thermal effect on the EOS is studied at temperature 5, 7, and 10 MeV. The EOS of supernova matter is found to be stiffer than the corresponding asymmetric nuclear matter equation of state as expected. Single particle properties like distribution functions and chemical potentials of proton, neutron, and electron are discussed for various values of electron fractions, densities, and temperatures. Distribution function is found to depend on Fermi kinetic energy of respective particles as well as on thermal energy. Chemical potential depends on number density of particles and temperature. It is also seen that the EOS for symmetric nuclear matter at low temperature has same order of magnitude with the recently extracted experimental values within the density range 0.35–0.56 fm^{-3}.

DOI: 10.1103/PhysRevC.75.015807 PACS number(s): 21.65.+f, 26.50.+x, 26.60.+c

I. INTRODUCTION

The fusion reaction in a massive star ($M > 8M_\odot$, where $M_\odot$ is the mass of the sun) continues till the light particles are exhausted and the core of the star consists of heavy elements like iron since iron has the highest binding energy per nucleon in periodic table. At this stage, the energy released by the nuclear reaction is not sufficient for further fusion reaction. As a result, the core begins to collapse. Once the densities of the central part of the core surpasses the normal nuclear matter density, the repulsive part of the nuclear force offers a powerful resistance for further compression. The shock waves so produced lead to a spectacular explosion resulting in the formation of a protoneutron star. It is short lived and very hot with a radius of about 100 km. It then contracts rapidly and within 0.1–1 second, quasihydrostatic equilibrium is reached where the radius drops from 100 km to about 10 km and the temperature falls. This stage is identified as the birth of a neutron star. At this stage, it is hot and composed of the so-called supernova matter characterized by a high and almost constant lepton fractions [1–3] with respect to nuclear matter densities and also by almost constant entropy per baryon [1]. Its maximum density would amount to several times normal nuclear matter density, $\rho_0 \simeq 2.7 \times 10^{14}$ g/cc^3 and the temperature is comparable to the Fermi energy of the constituents. Then it contracts gradually with the emission of neutrinos and evolves into a usual cold neutron star within 10–20 sec where the temperature falls to around 10^{-2} MeV. At this stage, the system consists of neutron star matter. It is speculated that matter at densities up to $\rho = 9\rho_0$ may be present in the interior of neutron star [4] and the matter at densities up to about $\rho = 4\rho_0$ may be present in the core collapse of type-II supernova [5]. The study of neutron star at its birth is of particular interest as it forms a new form of matter under extreme conditions.

There exist a few relativistic [6] and nonrelativistic [7–9] calculations for supernova matter. Several calculations for neutron star matter [10–13] are also available. Takatsuka *et al.* [8,9] have performed a detailed calculation for supernova matter within the frame work of finite temperature Hartree-Fock approach with effective nucleon-nucleon interaction (Reid-soft-core potential). They have considered electrons along with nucleons in one of their calculations [7] and then extended it to various compositions [8]. Sahu [12] has calculated the equation of state (EOS) of neutron star matter consisting of neutrons, protons, electrons, muons, and hyperons in relativistic mean field approximation at zero temperature. His EOS is moderately soft up to densities $\simeq 7\rho_0$. Vidaña *et al.* [13] have studied the EOS of β-stable neutron star matter in the frame work of Brueckner-Hartree-Fock approximation taking into account hyperons along with nucleonic degrees of freedom. Most of the above calculations are restricted to neutron star matter. Only a few microscopic calculations have been performed for supernova matter [7,8]. Gad [14] has studied the properties of neutron matter within the framework of Brueckner-Hartree-Fock approach using CD-Bonn and Bonn-C potentials. Danielewicz *et al.* [15] have recently analyzed the flow of matter in nuclear collisions and obtained constraints on the EOS of symmetric nuclear matter at zero temperature.

In the supernova implosion-explosion stage, neutrons outnumber the protons at the core. Hence to understand such matter, properties of asymmetric nuclear matter are important. Few years back we studied the properties of symmetric nuclear matter, pure neutron matter [16,17], and asymmetric nuclear matter [18,19] using density dependent Sussex interaction [20] at finite temperature in a fully self-consistent model. This model is a generalization of Brueckner theory to finite temperature in which scattering into intermediate states are

[*]Electronic address: rankasahu@rediffmail.com

taken into account. The degeneracy and the single particle potentials are calculated self-consistently. We successfully described the experimental observations [21] regarding the entropy production [16] in heavy-ion collisions. We have also explained the pion production [19] in asymmetric nuclear matter and liquid-gas phase transition in symmetric nuclear matter [17]. The success of our model has encouraged us to extend our calculation for the study of supernova matter. Here we have concentrated on the equation of state of supernova matter and the single particle properties like distribution function, chemical potential of its constituents at various values of densities, temperatures and electron fractions and compared them with the asymmetric nuclear matter EOS. Supernova matter is primarily composed of neutrons, protons, relativistic electrons, and degenerate electron neutrinos. Since the fraction of neutrinos is expected to be very small (<0.06 at low densities [1,3] and $\simeq 0.2$ at high densities [7]) we have neglected its contribution in our calculation. In Sec. II, we have briefly discussed our formalism. Section III contains the results and discussion. A brief summary of our work is presented in Sec. IV.

II. FORMALISM

We assume that the system under consideration is charge neutral. In our formalism, electrons are treated to be relativistic free particles and Coulomb interaction is neglected. Primarily supernova matter is concerned with asymmetric nuclear matter. We introduce the asymmetry parameter γ defined by $\gamma = n_+/n_-$, where n_+ is the number density of protons and n_- is the number density of neutrons. Since the density of protons and electrons are equal, we define the electron fraction y_e as $y_e = n_+/n$, where $n = n_+ + n_-$ is the number density of nucleons. Our asymmetry parameter and electron fraction is related as $\gamma = \frac{y_e}{1-y_e}$. The details of the formalism for nuclear matter were discussed in our earlier publications [17–19]. For completeness, here we give some important steps. In our formalism, we have extended the zero temperature Brueckner theory to finite temperature and started our formalism by writing the grand thermodynamic potential per unit volume,

$$\Omega = -P = -T \log \mathrm{tr}\, e^{-(H-\mu\hat{n})/T}, \tag{1}$$

where H and $\hat{n}$ are the Hamiltonian and number density operator. P, T, and μ are pressure, temperature, and chemical potential, respectively. The main reason for taking the grand thermodynamic potential lies in the fact that it can be expressed as a linked cluster expansion analogous to zero temperature Brueckner-Goldstone expansion, i.e.,

$$\Omega = \Omega_0 + \Omega_1 + \Omega_2 + \cdots, \tag{2}$$

where Ω_0, Ω_1, and Ω_2 are the contributions to the thermodynamic potential due to the unperturbed part, one-body part (single particle potential), two-body part of the Hamiltonian. Our formalism is limited up to Ω_2. In this formalism, we have used the Brueckner reaction matrix instead of the bare *NN* interaction. The number density of nucleon n_τ with isospin τ (+ for protons and − for neutrons) is given by

$$n_\tau = \frac{2}{(2\pi)^3} \int d^3k\, n_\tau(k) \tag{3}$$

$n_\tau(k)$ is the Fermi distribution function given by

$$n_\tau(k) = \frac{1}{1 + \exp\{[\epsilon_\tau(k) - \mu_\tau]/T\}}. \tag{4}$$

$\epsilon_\tau(k)$ is the single particle energy and μ_τ is the chemical potential of the nucleon. $\epsilon_\tau(k)$ is defined by

$$\epsilon_\tau(k) = \frac{\hbar^2 k^2}{2m_\tau} + U_\tau(k), \tag{5}$$

where $U_\tau(k)$ is the single particle potential and is defined by

$$U_+(k_1) = \frac{1}{2\pi^2} \int_0^\infty dk_2 [n_+(k_2) g_{++}(E_s, k_1, k_2) + n_-(k_2) g_{-+}(E_s, k_1, k_2)]. \tag{6}$$

The g's are the interaction matrices,

$$g_{\tau\tau'}(E_s, k_1, k_2) = \frac{\arctan[\pi \rho_E Q_{\tau\tau'} K_{\tau\tau'}(E_s)]}{\pi \rho_E Q_{\tau\tau'}}. \tag{7}$$

Here ρ_E is the single particle level density and the K matrix satisfies the integral equation

$$K_{\tau\tau'}(E_s) = V_{\tau\tau'} + V_{\tau\tau'} \frac{Q_{\tau\tau'}}{E_s - H_0} K_{\tau\tau'}, \tag{8}$$

$V_{\tau\tau'}$ is the realistic nuclear interaction, $Q_{\tau\tau'}$ is the Pauli operator, and E_s is the starting energy of the two particles. In our calculation, we have used two-body density dependent Sussex interaction [20]. The parameters of the density dependent term of this interaction are determined empirically [20] by fitting the binding energies and densities of nuclear matter and ^{16}O. For a given value of nuclear matter density and electron fraction, we fix the number density of proton and neutron. Then chemical potential is calculated from the number density constraint. The single particle potential is needed for the calculation of the single particle potential itself. Ultimately the single particle potential is calculated by the iteration method. Thus, in our formalism, self-consistency is satisfied with respect to the single particle potential and chemical potential.

Internal energy per nucleon and pressure for nuclear matter are calculated using the following expressions:

$$\epsilon_n = \frac{1}{n} \sum_\tau \frac{2}{(2\pi)^3} \int_0^\infty d^3k n_\tau(k) \left(\frac{\hbar^2 k^2}{2m_\tau} + \frac{1}{2} U_\tau(k) \right), \tag{9}$$

$$P_n = \frac{1}{\pi^2} \sum_\tau \int_o^\infty dk k^2 n_\tau(k) \left(\frac{1}{3} k \frac{d\epsilon_\tau}{dk} + \frac{1}{2} U_\tau(k) \right). \tag{10}$$

It was been mentioned earlier that the electron fraction is equal to the proton fraction and electrons are considered as relativistic free particles. The single particle energy of the electron is given by

$$\epsilon_e(k) = \sqrt{\left(k^2 + m_e^2\right)}, \tag{11}$$

where m_e is the mass of the electron. The distribution function for the electron is calculated using an expression similar to that of a nucleon. Its chemical potential is also calculated using the number density constraint. The internal energy per nucleon and pressure for electrons are calculated using the following expressions:

$$\epsilon_{el} = \frac{2}{n(2\pi)^3}\int_0^\infty d^3k\; n_e(k)\epsilon_e(k), \tag{12}$$

$$P_{el} = \frac{1}{3\pi^2}\int_0^\infty \frac{k^2}{\left(k^2+m_e^2\right)^{\frac{1}{2}}} n_e(k)k^2 dk, \tag{13}$$

where $n_e(k)$ is the distribution function for the electron. Total energy per nucleon and pressure of the supernova matter are given by

$$\epsilon = \epsilon_n + \epsilon_{el}, \tag{14}$$

$$P = P_n + P_{el}. \tag{15}$$

III. RESULTS AND DISCUSSION

We have plotted the internal energy per nucleon in Fig. 1 for supernova matter and asymmetric nuclear matter at various values of densities for proton/electron fractions $y_p = 0.1$ and 0.3 at temperatures 5, 7, and 10 MeV. We find that at a given temperature, as the proton concentration y_p increases, energy per nucleon for nuclear matter decreases at low density region. But it increases when density becomes higher. On the other hand, in the case of supernova matter, as proton concentration increases, energy per nucleon increases for all the values of densities and the curve becomes stiffer. It seems that in nuclear matter, the strong nuclear interaction overcomes the kinetic energy at low density region and causes its bound state. But in the high density region, gain in momentum dominates over this interaction resulting in the increase of energy per nucleon. In the case of supernova matter, kinetic energy of relativistic electrons predominates over the strong nuclear interactions in this low density region and surpasses the kinetic energy of nuclear matter in the high density region which enhances the energy per nucleon at all the densities. We also observe that the EOS of supernova matter is stiffer than that of asymmetric nuclear matter. We also find that as the thermal energy is enhanced, the energy per nucleon for both matter is enhanced. This may be due to the conversion of thermal energy into kinetic energy leading to an increase of energy per nucleon. The contribution of electron energy in enhancing the energy per nucleon is larger than that of thermal energy. As has been discussed before, a similar type of calculation has been performed by Takatsuka [7]. He has calculated the energy per nucleon of supernova matter within the framework of finite temperature Hartree-Fock approximation using the Reid soft core potential taking into account the electrons along with nucleons. From his studies he came to the conclusion that the EOS of supernova matter is remarkably stiffer and the contribution of electron energy in this stiffening effect of EOS is larger than that of thermal energy, similar to the result of our calculation.

Recently Danielewicz *et al.* [15] have tried to determine experimentally the EOS of dense nuclear matter from the collision between ^{197}Au and ^{197}Au nuclei at incident kinetic energy ranging from 0.15 to 10 GeV per nucleon. They analyzed the transverse flow of matter in nuclear collision and extracted the pressure at high densities and at zero temperature. We have plotted our results for pressure for symmetric nuclear matter at temperature $T = 10$, 20, and 30 MeV in Fig. 2 and compared our results with their experimentally extracted value. The closed region in this figure gives the experimental values of the pressure as a function of densities for symmetric nuclear matter. Our EOS of symmetric nuclear matter within the density range 0.35–0.56 fm^{-3} and in these low temperature limits has the same order of magnitude as the experimental values.

Our results for pressure at various values of densities are plotted in Fig. 3 for supernova matter and asymmetric nuclear matter at temperature 5, 7, and 10 MeV for $y_p = 0.1$ and 0.3. We have also plotted the pressure at temperature 20 and 30 MeV in the same figure just to compare the thermal effect. The dotted curves represent the supernova matter and solid curves represent the asymmetric nuclear matter. We observe that for a given proton fraction, say for $y_p = 0.1$, the pressure

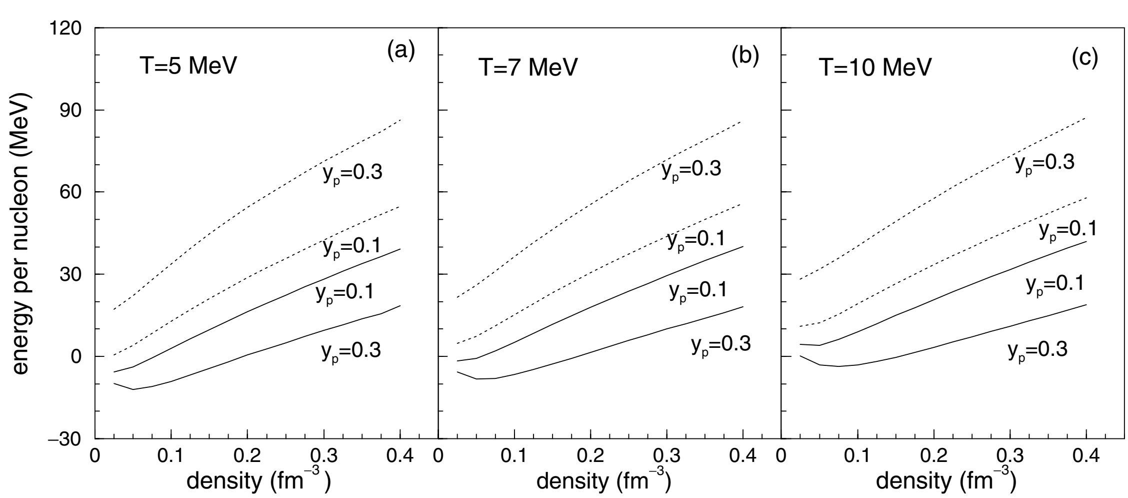

FIG. 1. Internal energy per nucleon for nuclear matter (solid line) and supernova matter (dotted line) at temperatures 5, 7, and 10 MeV (for supernova matter $y_p = y_e$).

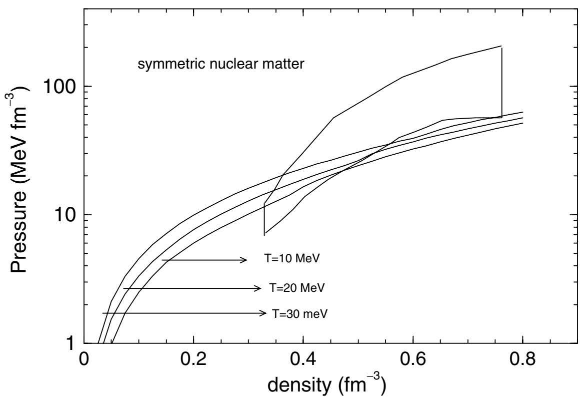

FIG. 2. Pressure versus density for symmetric nuclear matter at temperatures 10, 20, and 30 MeV. Experimental results are shown in closed region.

curves of asymmetric nuclear matter at temperature $T = 5$, 7, and 10 MeV coincide in the high density region. It seems that pressure curves are degenerate in this region. In the low density region, the thermal effect is negligible. We also obtain a similar type of pressure curves for supernova matter. For this matter, pressure is slightly higher than that of nuclear matter. This may be due to the presence of the electron in this matter. When the temperature is increased to 20 and 30 MeV, the thermal effect in the low density region is prominent for both the matter and its effect is reduced as density goes up. It may be due to the fact that in low density region, the temperatures $T = 5, 7,$ and 10 MeV are comparable to Fermi kinetic energy of the constituents of the system and due to the small contribution of the nuclear interaction energy. In the high density region, as momentum gain is there, the above temperatures are not comparable to the kinetic energy. So in this region, there is no contribution of thermal energy. As the temperature increases to 20 and 30 MeV, thermal energy becomes larger than the Fermi kinetic energy in the low density region and hence the effect of thermal energy is dominant. In the high density region, thermal energy is not sufficient enough over the Fermi kinetic energy. When the

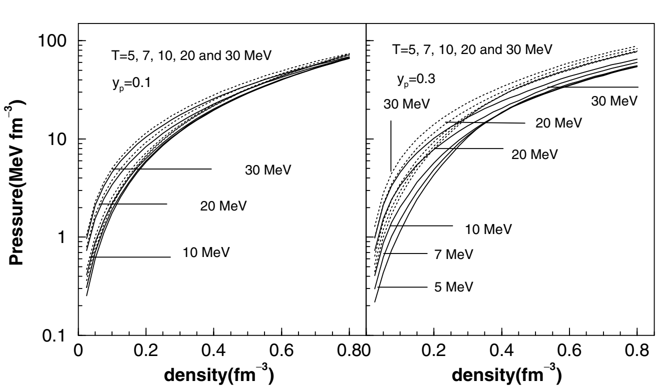

FIG. 3. Pressure versus density for nuclear matter (solid line) and supernova matter (dotted line) at temperatures 5, 7, 10, 20, and 30 MeV.

proton fraction is increased from 0.1 to 0.3, the thermal effect is prominent in the low density region for both the nuclear matter and supernova matter at temperature $T = 5$, 7, and 10 MeV. In the high density region and within these temperatures the pressure curves are also degenerate for both matter. We also find that there is a reduction of pressure by a small amount in the case of nuclear matter and increase of pressure for supernova matter at a constant density. It may be due to the enhanced contribution of the nuclear interaction energy which reduces the pressure in nuclear matter. On the other hand, the enhanced electron fraction leads to slight increase in pressure for supernova matter. When the temperature is increased to 20 and 30 MeV, thermal effects are enhanced in the low density region and it slows down as density increases. However the pressure is larger for supernova matter. This larger value of pressure for supernova matter is mainly due to the presence of the additional fraction of electrons. It is well known that at a given temperature, the pressure is proportional to the number of particles per unit volume regardless of the size of the individual particles. So the electrons present in supernova matter contribute additional pressure to this matter which also enhances the stiffness of its EOS.

Distribution functions for proton, neutron, and electron at various values of momenta for densities $\rho = \rho_0$ and $2\rho_0$ and for electron fractions $y_e = 0.1$ and 0.3 at temperature 10, 20, and 30 MeV are plotted in Fig. 4. Here we observe that for a given temperature, density, and electron fraction, say for $y_e = 0.1$, the probability of the distribution for proton is less than that of the neutron and electron. It shows that the proton is more diffused. We also observe that though the fraction of protons and electrons are the same, the probability of the distribution for both the particles is not equal. This discrepancy may be due to the thermal effect of the respective particles. The thermal effect is defined [8] as the ratio of thermal energy to the Fermi kinetic energy of the concerned particles. For example, for $\rho = \rho_0$ and $y_e = 0.1$, $\rho_p = \rho_e = 0.0165$ fm^{-3}, and $\rho_n = 0.1485$ fm^{-3} and correspondingly Fermi kinetic energies of the proton, neutron, and electron are 12.8, 55.0, and 155.37 MeV, respectively. Thus, even though the densities of the protons and electrons are equal, the thermal effect of the protons is larger than that of electrons for a given temperature and density. As we go to a higher fraction of electrons say from $y_e = 0.1$ to $y_e = 0.3$, at a given density and temperature, we find that the probability of distribution for the proton is affected substantially. The distribution function for protons and electrons increases but for neutrons, it decreases. Here on an increasing proton fraction, its density in matter increases which results in increasing its Fermi kinetic energy. As a result, at constant temperature and density, its thermal effect is reduced leading to increase in its probability of distribution. We also observe that the proton and electron distribution curves cross each other at a point for a given value of electron fraction. For example in Fig. 4(a), we find that at temperature 10 MeV, for $\rho = \rho_0$ and electron fractions $y_e = 0.1$ and 0.3, the crossing points are at 0.79 and 1.14 fm^{-1}. These values nearly correspond to the Fermi momentum of proton/electron in their respective electron fractions. On increasing the temperature and density, these crossing points attain higher values. The nature of the distribution function of the proton, neutron, and

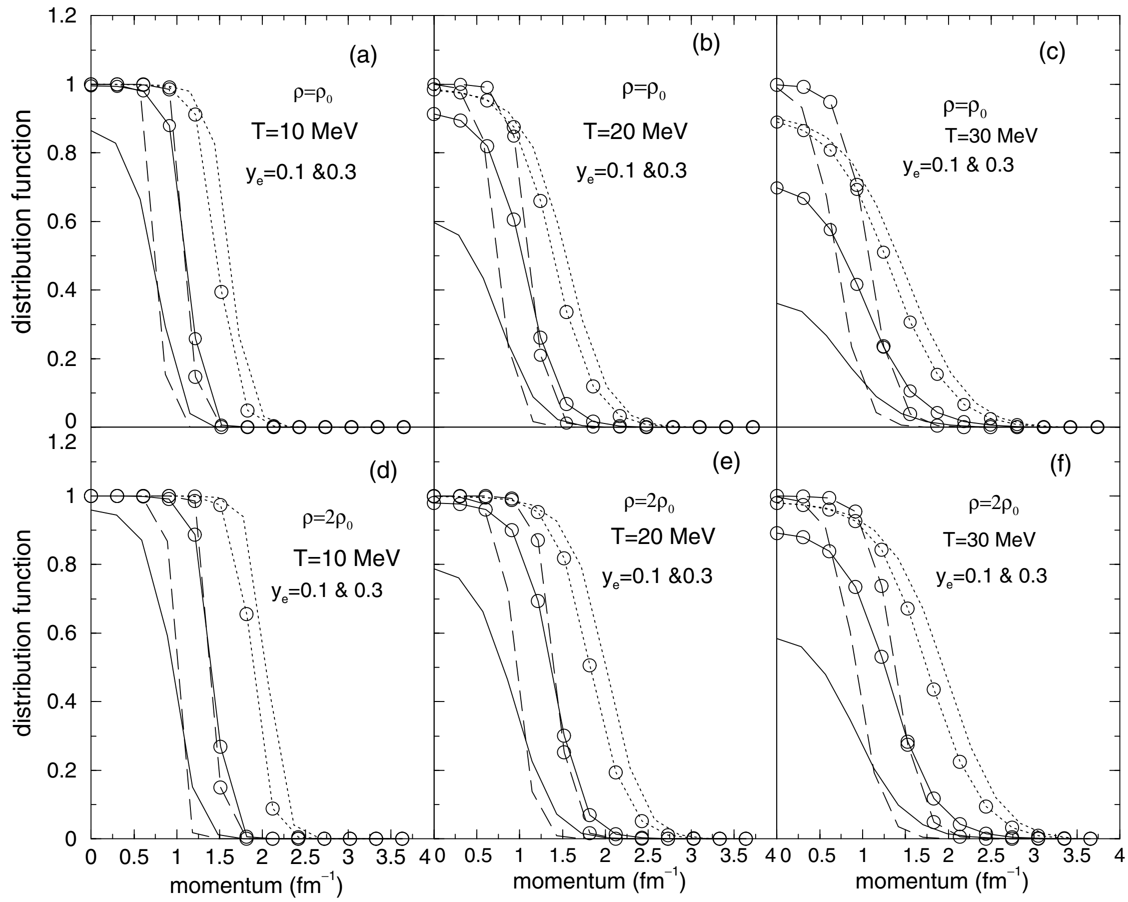

FIG. 4. Distribution function of the proton (solid line/solid line with circles), neutron (dotted line/dotted line with circles), and electron (long-dashed line/long-dashed line with circles) for electron fraction ($y_e = 0.1/y_e = 0.3$) are plotted at various values of momenta at temperatures 10, 20, and 30 MeV and at $\rho = \rho_0$ and $\rho = 2\rho_0$.

electron agrees well with the calculation made by Takatsuka *et al.* [8], where they have considered the β-equilibrium. The distribution functions for density $\rho = 2\rho_0$ at various values of temperatures are given in Figs. 4(d)–4(f). Comparing the Figs. 4(a)–4(c) with that of Figs. 4(d)–4(f), we observe that at a given temperature, the probability of the distribution for all

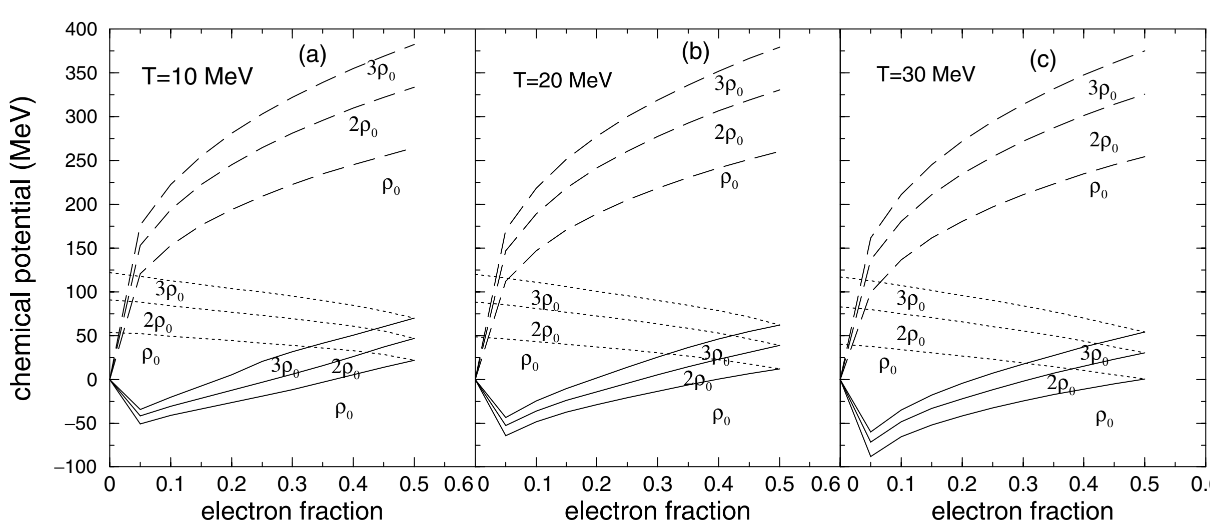

FIG. 5. The chemical potential of the proton (solid line), neutron (dotted line), and electron (long-dashed line) are plotted for various values of electron fractions at temperatures 10, 20, and 30 MeV.

the particles increases as the density of the system increases. As explained before, this increase in the distribution function is due to the decrease in thermal effect which is the ratio of thermal energy to Fermi kinetic energy.

In Fig. 5, we have plotted the chemical potential for the proton, neutron, and electron for various values of electron fractions as well as densities at temperatures 10, 20, and 30 MeV. We observe that for a given temperature, there is a sharp fall of the chemical potential of the proton up to the electron fraction 0.05 and then it increases. But in the case of the electron, there is a sharp increase in chemical potential up to this electron fraction and then the increase tapers off. On the other hand in the case of neutrons, the chemical potential decreases slowly for all values of electron fractions. As is evident from the graph, the chemical potential of protons and neutrons is equal for symmetric nuclear matter which corresponds to the electron fraction $y_e = 0.5$. We also observe that the chemical potential of the electron is much larger than that of the proton at a given density and temperature. It may be due to the relativistic nature of the electron. It is seen that as the density of the system increases from ρ_0 to $3\rho_0$, the chemical potential of all particles increases for all values of electron fractions. It shows that the enhancement of the chemical potential depends upon the enhancement of Fermi momentum. We also find that the thermal energy has very little effect on chemical potential. Our results are similar to those of Takatsuka *et al.* [8].

IV. CONCLUSION

We have performed a nonrelativistic microscopic calculation for the equation of state of supernova matter consisting of protons, neutrons, and electrons in the framework of Brueckner-Goldstone expansion using the density dependent two-body Sussex interaction and compared the results with those of asymmetric nuclear matter and studied the thermal effect on it. It is observed that in the low density region, the temperatures 5, 7, and 10 MeV are comparable to Fermi energies and hence there are contributions at these temperatures. But in the high density regions, these temperatures have no contribution on pressure for both matter. Even though our calculated EOS is at finite temperature, we have compared our results of symmetric nuclear matter with the recently extracted values of EOS at zero temperature [15] since we restrict our results to low temperatures. The agreement is satisfactory within the density range 0.35–0.56 fm^{-3}. We observe that the EOS of supernova matter is stiffer than the EOS of nuclear matter. In this stiffening effect, the relativistic nature of the electrons plays the dominant role. We also observe that the contribution of electron energy is remarkably larger than that of thermal energy. We studied the single particle properties of the constituents of supernova matter. For a given temperature, density, and electron fraction, the probability of the distribution for the proton is less than that of neutron and electron. Though the density of the proton and electron are equal, their probability of distribution are not equal. It mainly depends upon thermal energy and Fermi kinetic energy. We find that there is a sudden fall and rise of the chemical potential for the proton and electron up to electron fraction 0.05. Beyond this value of the electron fraction, the chemical potential of the proton and electron increases. But in the case of neutron chemical potential, the above type of behavior is absent and this potential decreases slowly as the fraction of electron increases. The chemical potential for all these particles increase as density of the system increases.

We find that our calculation does not satisfy the Hugenholtz-Van Hove theorem. However Baldo *et al.* [22] and Grange *et al.* [23] have shown that, with the inclusion of the rearrangement term, this theorem is satisfied for symmetric nuclear matter at different temperatures. We plan to carry out this study in the future.

In the future we also plan to carry out the above calculations with other interactions like the Bonn and Paris potentials and try to see the effect of interactions on the properties of supernova matter.

ACKNOWLEDGMENTS

This work has been partially supported by the Department of Science and Technology, Govt. of India, New Delhi.

[1] H. A. Bethe, G. E. Brown, J. Applegate, and J. M. Lattimer, Nucl. Phys. **A324**, 487 (1979).
[2] R. I. Epstein and C. J. Pethick, Astrophys. J. **243**, 1003 (1981).
[3] J. M. Lattimer, C. J. Pethick, D. G. Ravenhall, and D. Q. Lamb, Nucl. Phys. **A432**, 646 (1985).
[4] J. M. Lattimer and M. Prakash, Astrophys. J. **550**, 426 (2001).
[5] H. A. Bethe, Rev. Mod. Phys. **62**, 801 (1990).
[6] H. Shen, H. Toki, K. Oyamatsu, and K. Sumiyoshi, Nucl. Phys. **A721**, 1048 (2003).
[7] T. Takatsuka, in *Structure and Evolution of Neutron Star*, edited by D. Pines, R. Tamagaki, and S. Tsumuta (Addison-Wesley, 1992), p. 257 and references therein.
[8] T. Takatsuka, S. Nishizaki, and J. Hiura, Prog. Theor. Phys. **92**, 779 (1994).
[9] T. Takatsuka, Prog. Theor. Phys. **95**, 901 (1996).
[10] I. Vidaña, A. Polls, A. Ramos, L. Engvik, and M. Hjorth-Jensen, Phys. Rev. C **62**, 035801 (2000).
[11] C. H. Hyan, M. H. Kim, and S. W. Hong, Nucl. Phys. **A718**, 709c (2003).
[12] P. K. Sahu, Phys. Rev. C **62**, 045801 (2000).
[13] I. Vidaña, I. Bombaci, A. Polls, and A. Ramos, Nucl. Phys. **A719**, 173c (2003).
[14] Kh. Gad, Nucl. Phys. **A747**, 655 (2005).
[15] Powel Danielewicz, Roy Lacey, and William, G. Lynch, Science **298**, 1592 (2002).
[16] C. Das, R. K. Tripathi, and J. Cugnon, Phys. Rev. Lett. **56**, 1663 (1986).

[17] C. Das, R. K. Tripathi, and R. Sahu, Phys. Rev. C **45**, 2217 (1992).
[18] C. Das and R. Sahu, Phys. Lett. **B289**, 217 (1992).
[19] C. Das, R. Sahu, and R. K. Tripathi, Phys. Rev. C **48**, 1056 (1993).
[20] R. K. Tripathi, J. P. Elliot, and E. A. Sanderson, Nucl. Phys. **A380**, 483 (1982).
[21] B. V. Jacak, G. D. Westfall, C. K. Gelbke, L. H. Harwood, W. G. Lynch, D. K. Scott, H. Stoeker, M. B. Tsang, and T. J. M. Symons, Phys. Rev. Lett. **51**, 1846 (1983).
[22] M. Baldo, I. Bombaci, L. S. Ferreira, G. Giansiracusa, and U. Lombardo, Phys. Lett. **B215**, 19 (1988).
[23] P. Grange, J. Cugnon, and A. Lejeune, Nucl. Phys. **A473**, 365 (1987).